of Phe 120 (RNase A/CpA simulations) and from NE2 of Gln 11 (RNase/deoxy-CpA crystal structure) as well as from water molecules to the phosphoryl oxygens. These interactions with the phosphoryl oxygens are expected to facilitate the reaction by polarizing the phosphate and making it more susceptible to nucleophilic attack.

Present throughout the reaction are hydrogen bonds from ND1 of His 12 to the backbone O of Thr 45, from Asp 121 to the backbone of Lys 66, from the NH backbone of Phe 120 and/or from NE2 of Gln 11 to the phosphoryl oxygens. In addition, water molecules in the active site provide partial solvation of the lysines, the phosphate, and Asp 121. The calculations indicate that Lys 7 does not hydrogen bond to the substrate or participate directly in the reaction. On the other hand, Lys 66 and Asp 121 may have important roles; this is also suggested by chemical modification studies of these residues.

The simulations reported here represent only one step in an analysis of the reaction dynamics of RNase A. It is hoped that ab initio calculations of the reaction path[38] and additional molecular dynamics simulations that are in progress will enable us to address other questions that need to be answered for a full understanding of the detailed dynamics of RNase catalysis.

Acknowledgment. We thank G. Petsko for supplying the crystal coordinates used in this paper and many helpful discussions. We are grateful to the Minnesota Supercomputing Centre and Cray Research Laboratory at Mendota Heights for the use of their computing facilities, and we thank Dr. Eric Wimmer, Dr. John Mertz, Dr. Chris Haydock, and the computing staff at CRL for their assistance.

(38) Lim, C.; Karplus, M. *J. Am. Chem. Soc.* Submitted for publication.

Thiol Surface Complexation on Growing CdS Clusters†

V. Swayambunathan,‡ David Hayes,‡ Klaus H. Schmidt,‡ Y. X. Liao,§ and Dan Meisel*,‡

Contribution from the Chemistry Division and Material Sciences Division, Argonne National Laboratory, Argonne, Illinois 60439. *Received March 3, 1989*

Abstract: The growth of small CdS colloidal particles has been initiated by pulse radiolytic release of sulfide from a thiol (3-mercapto-1,2-propanediol, RSH) in the presence of Cd^{2+} ions. The kinetics and stoichiometry of the ensuing reactions were followed by conductivity, absorption spectroscopy, and light-scattering techniques. The final CdS product has been identified by electron diffraction. The formation of Cd-thiolate complexes at the surface of the particles is indicated by conductivity and by energy dispersive analysis of X-ray (EDAX) results. The rate of formation of CdS clusters is strongly pH dependent due to the pH effect on the stability of Cd^{2+}/HS^- complexes. At low pHs (4.0-5.3) the growth mechanism is proposed to be primarily a cluster-molecule process. At this pH range Cd^{2+} ions at the CdS particle surface complex with thiolate ions stronger than in the bulk of the solution. The size control of the particles by thiols is proposed to result from a competition of thiolate ions with HS^- ions for cadmium ions at the surface of the growing particles. At neutral and basic pHs growth is primarily a cluster-cluster aggregation process of CdS clusters within the cadmium-thiolate polynuclear complexes. The small particles seem to undergo weak clustering in solution, yet the spectroscopic properties of the samll particles is maintained. The utility of the thiol-controlled growth, both in size control and surface modification, is discussed.

Studies of the spectroscopic and photocatalytic properties of semiconductors in colloidal state have gained popularity in recent years, in particular following the observation of the dependence of these properties on size.[1,2] Consequently, much effort has been expended in the synthesis of these small, quantum size particles. Among the various semiconductor materials, those of the II-VI groups, and especially cadmium chalcogenides, drew much of the attention. Prerequisite for systematic studies of quantum size effects is a general procedure to synthetically control the size of the particles. Particles of CdS were successfully synthesized in a variety of media such as non-aqueous solvents,[1,3] reversed micelles,[4] vesicles,[5] polymer films,[6] and zeolites.[7,8] The work of Nosaka et al.,[9] has demonstrated the remarkable ability of thiols to stabilize small particles. Recently, we synthesized small CdS particles by γ-radiolysis of thiols in the presence of Cd^{2+} ions.[10] It was shown that in addition to serving as a source of sulfide ions, the thiols also play an important role as growth moderators. The latter property was attributed to the ability of thiolate anions (and polynuclear complexes between cadmium ions and thiolate ions) to bind strongly to cadmium ions at the particle surface, thereby effectively inhibiting further growth of small CdS particles. Surface modification of CdSe particles, which also prevents further agglomeration, has been recently demonstrated by Brus and coworkers in organic solvents using a multistep organometallic synthetic procedure.[11]

The ability to prepare particles of systematically controlled sizes as a result of a surface complexation reaction process is very appealing. In this paper, we report our results on the formation and properties of colloidal CdS particles from the very early stages of their existence in solution using the pulse radiolysis technique. An advantage of the radiation initiation approach is the ability to study the growth process essentially without any limitations of time resolution. This was demonstrated earlier in a study of silver halides growth.[12] The procedure adopted here is similar

† Work performed under the auspices of the Office of Basic Energy Sciences, Division of Chemical Science, US-DOE under contract No. W-31-109-ENG-38.

‡ Chemistry Division.
§ Material Sciences Division.

(1) Henglein, A. *Top. Curr. Chem.* **1988**, *143*, 113.
(2) Brus, L. E. *J. Phys. Chem.* **1986**, *90*, 2555.
(3) Ramsden, J. J.; Webber, S. E.; Grätzel, M. *J. Phys. Chem.* **1985**, *89*, 2740.
(4) Lianos, P.; Thomas, J. K. *Chem. Phys. Lett.* **1986**, *125*, 299.
(5) Watzke, H. J.; Fendler, J. H. *J. Phys. Chem.* **1987**, *91*, 854.
(6) Wang, Y.; Suna, A.; Mahler, W.; Kasowski, R. J. *J. Phys. Chem.* **1987**, *87*, 7315.
(7) Stramel, R. D.; Nakamura, T.; Thomas, J. K. *J. Chem. Soc., Faraday Trans I* **1988**, *84*, 1287.
(8) Wang, Y.; Herron, N. *J. Phys. Chem.* **1987**, *91*, 257.
(9) Nosaka, Y.; Yamaguchi, K.; Miyama, H.; Hayashi, H. *Chem. Lett.* **1988**, 605.
(10) Hayes, D.; Micic, O. I.; Nenadovic, M. T.; Swayambunathan, V.; Meisel, D. *J. Phys. Chem.* **1989**, *93*, 4603.
(11) Steigerwald, M. L.; Alivisatos, A. P.; Gibson, J. M.; Harris, T. D.; Kortan, R.; Muller, A. J.; Thayer, A. M.; Duncan, T. M.; Douglass, D. C.; Brus, L. E. *J. Am. Chem. Soc.* **1988**, *110*, 3046.

0002-7863/90/1512-3831$02.50/0

Table I. Relevant Rate Constants for Radiolytically Produced Radicals with RSH and Cd^{2+} [a]

eq. no.	reaction	k, M^{-1} s^{-1}
1	$e^-(aq) + RSH \rightarrow R + HS^-$	6.0×10^9 [b]
2	$OH + RSH \rightarrow RS + H_2O$	6.8×10^9
3	$H + RSH \rightarrow RS + H_2$	1.4×10^9
4	$e^-(aq) + Cd^{2+} \rightarrow Cd^+$	5.5×10^{10}
5	$OH + Cd^{2+} \rightarrow$ products	$<5 \times 10^5$
6	$H + Cd^{2+} \rightarrow$ products	$<3 \times 10^5$

[a] Unless otherwise stated, 2-mercaptoethanol is used as a representative RSH compound. Values taken from the compilations of: Buxton, G.; Greenstock, C. L.; Helman, W. P.; Ross, A. B. *J. Phys. Chem. Ref. Data* **1988**, *17*, 513. Rate Constants for Reactions of Inorganic Radicals in Aqueous Solutions. Neta, P.; Huei, R. E.; Ross, A. B. *J. Phys. Chem. Ref. Data*, in press. [b] This work, measured for 3-mercapto-1,2-propanediol.

to the earlier γ-radiolysis experiments, i.e., sulfide ions were generated by the dissociative addition of solvated electrons to 3-mercapto-1,2-propanediol (RSH). The evolution of the absorption spectrum of such particles was monitored from the moment the radiation pulse was applied to the solution. Measurements of the conductivity changes of the solution provide quantitative information on the stoichiometry and some information on the kinetics of the growing particles. Light-scattering measurements and transmission electron microscopy (TEM) provide complementary information on the sizes of the particles. The crystal structure of the particles was obtained from analysis of electron diffraction patterns, and evidence for the binding of thiolate ions to cadmium ions at the surface of the particles is presented. This in turn suggests strategies for the production of surface-modified particles.

Experimental Section

The pulse radiolysis systems used in the present study have been previously described.[12] Electron pulses of 4 ns–3.0 μs width were used to generate sulfide ions in the concentration range of 2.5×10^{-6}–2.2×10^{-4} M. Conductivity changes following the irradiation pulse were monitored with use of a pulsed DC technique for short times (<1 ms) and an AC technique for longer times. Absorption spectra were recorded with the streak camera system as previously described.[12b] For light-scattering measurements a 5mW He–Ne laser (Hughes Model 3225H-PC) was used for excitation and the scattered light was collected at 90° to the excitation and polarization planes. The procedure and assumptions involved in converting the scattered light signal to the Rayleigh parameter and to volume weighted average volumes have been discussed in detail.[12b] For the present calculations bulk density $\rho = 4.82$ g/cm^3 and index of refraction $n_p = 2.560$ of CdS were assumed.

The solutions used for irradiation typically contained the thiol, 3-mercapto-1,2-propanediol (RSH), and $CdSO_4$ and were deaerated with use of the syringe technique. $HClO_4$ or NaOH were added to adjust the pH. Conductivity measurements were carried out in the absence of any buffer in the pH range 4.0–5.3. The streak camera and light scattering experiments were carried out at pH 4.2 and 7.0, the latter in the presence of 10^{-4} M phosphate buffer. TEM studies were conducted with a JEOL 100CX or a Philips EM420 machine equipped with EDAX accessories. For these measurements, the samples were deposted on 400-mesh copper grids coated with 50-Å carbon film.

Results and Discussion

Table I summarizes the reactions that occur upon irradiation of aqueous solutions of thiols (reactions 1–3) and their relevant rate parameters.[10,13] Also included are the corresponding reactions of Cd^{2+} (reactions 4–6). The reactions of interest are reaction 1 in the table and those of HS^- following its release from the thiol. Competition between the thiol and Cd^{2+} for e_{aq}^- was minimized by the choice of their concentrations. Production of Cd^+ via the competing reaction 4 (Table I), while easily observable in the absorption spectra at early times, had no effect on the colloidal CdS produced, except to reduce its yield. With use of the known rate constants and concentrations, corrections for this competition, as well as competition by protons, were applied when necessary. The OH radicals reacted with RSH in the presently studied solutions. It was verified, by irradiation of appropriate blank solutions, that neither the thiyl radicals, produced in reactions 2 and 3, nor any other irradiation product (e.g. hydrogen peroxide, produced in small quantities on irradiation of aqueous solutions) has any effect on the results reported below.

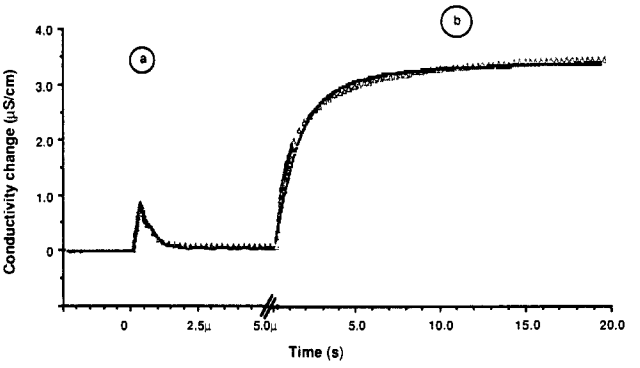

Figure 1. Time profile of conductivity signals following the pulse radiolysis of 4.0×10^{-5} M Cd^{2+}, 1×10^{-2} M RSH deaerated solution at pH 4.0. $[H_2S]_0 = 6.1 \times 10^{-6}$ M. (a) At short times, release and protonation of HS^-. (b) At longer times, release of protons upon formation of CdS. Solid curve: experimental results. Triangles: computer simulation as described in text.

a. Release and Protonation of HS^-. The release of HS^- from RSH via reaction 1 and its protonation rate, reaction 7, were

$$e_{aq}^- + RSH \rightarrow R + HS^- \quad (1)$$

$$HS^- + H^+ \rightleftharpoons H_2S \quad (7)$$

measured with use of the conductivity technique in the pH range 4.0–5.3 (for H_2S, $pK_{a1} = 7.0$, and for RSH, $pK_a = 9.43$[14]). The conductivity signal immediately after the pulse (Figure 1a) reflects primarily the increase in conductance due to the protons produced by the radiolysis of water and the release of HS^- (reaction 1 is essentially complete during the pulse at the concentrations used). The rate of the decay of this signal, due to reaction 7, was found to be linear with proton concentration in this pH range, yielding $k_7 = 2.9 \times 10^{10}$ M^{-1} s^{-1}. From the pK_a and k_7 one calculates for the back reaction $k_{-7} = 2.9 \times 10^3$ s^{-1}. Plots of the pseudo-first-order rate constants vs $[H^+]$, however, yielded a non-zero intercept. This intercept is attributed to the protonation of HS^- by its reaction with water. The bimolecular rate constant for the latter reaction was calculated from the intercept to be 6.6×10^3 M^{-1} s^{-1}. At the end of the decay the amplitude of the conductivity signal returned, within a few percent, to the prepulse level. The residual small conductivity signal quantitatively agrees with the amount of dissociated H_2S calculated from equilibrium 7.

In the pH range 4.0–5.3 and at the Cd^{2+} concentrations used ($\leq 2 \times 10^{-4}$ M), the latter does not compete with protons for HS^-, and protonation (reaction 7) dominates. This, however, is not an indication that the reaction of cadmium ions with HS^- (reaction 8) is slow. On the contrary, in accordance with Eigen's model,[15]

$$Cd^{2+} + HS^- \rightleftharpoons CdHS^+ \quad (8)$$

we believe that reaction 8 is diffusion controlled. However, the stability constant of the $CdHS^+$ complex is small enough to shift equilibrium 8 to the left at the pHs studied. Whereas the stability constant for equilibrium 8 has been reported to be 4.0×10^7,[16]

(12) (a) Schmidt, K. H.; Patel, R. C.; Meisel, D. *J. Am. Chem. Soc.* **1988**, *110*, 4882. (b) Hayes, D.; Schmidt, K. H.; Meisel, D. *J. Phys. Chem.* **1989**, *93*, 6100.

(13) (a) Swallow, A. J. *Prog. React. Kinet.* **1978**, *9*, 195. (b) Wardman, P. In *Radiation Chemistry*; Farhataziz, Rodgers, M. A. J., Eds.; VCH Publishers: Weinheim, FRG, 1987; p 593. (c) Lal, M.; Armstrong, D. A. *Can. J. Chem.* **1985**, *63*, 30.

(14) De Brabander, H. F.; Van Poucke, L. C. *J. Coord. Chem.* **1974**, *3*, 301.

(15) (a) Eigen, M. *Ber. Bunsenges. Phys. Chem.* **1963**, *67*, 753. (b) Diebler, H.; Eigen, M.; Ilgenfritz, G.; Maas, G.; Winkler, R. *Pure Appl. Chem.* **1969**, *20*, 93.

(16) Ste-Marie, J.; Torma, A. E.; Gubeli, A. O. *Can. J. Chem.* **1964**, *42*, 662.

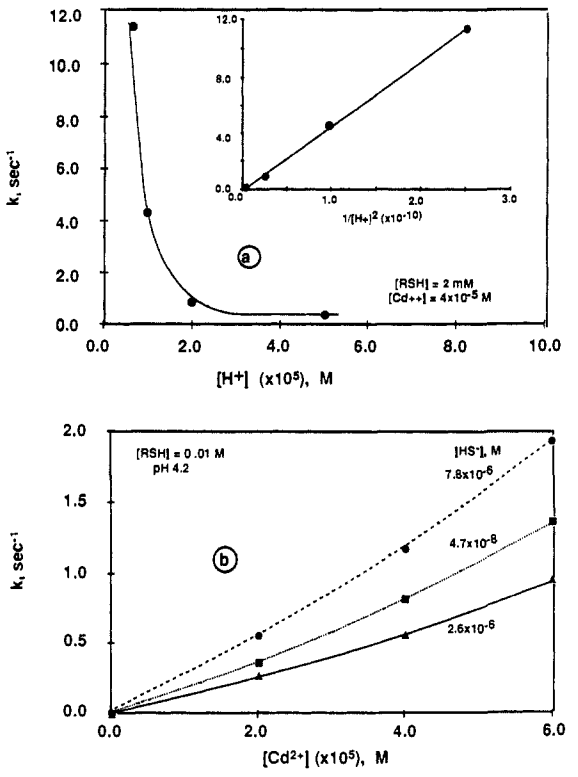

Figure 2. Effect of $[H^+]$, $[Cd^{2+}]_o$, and $[H_2S]_o$ on rate of proton release upon formation of CdS. (a) Effect of $[H^+]$; [RSH] = 2×10^{-3} M; $[Cd^{2+}] = 4 \times 10^{-5}$ M; $[H_2S]_o = 3.0 \times 10^{-6}$ M. Insert: Dependence of observed rate constant on $1/[H^+]^2$. (b) Effect of $[Cd^{2+}]_o$; [RSH] = 1×10^{-2} M at pH 4.2 for various $[H_2S]_o$.

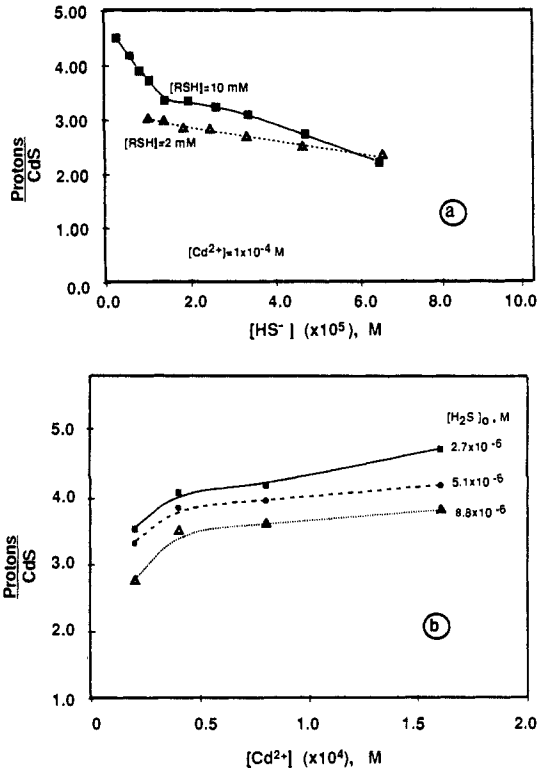

Figure 3. Number of protons released per CdS molecule formed (assuming all H_2S reacted with Cd^{2+}) at the end of the reaction as a function of (a) $[H_2S]_o$, at constant Cd^{2+} for two RSH concentration, and (b) $[Cd^{2+}]_o$, in 1×10^{-2} M RSH, for three $[H_2S]_o$. All solutions were Ar saturated at pH 4.1. Other experimental conditions are indicated in the figure.

we will show here that such a high value is incompatible with our results at longer time scales.

b. The Reaction of Cd^{2+} with H_2S. From the previous section we conclude that in the acidic range most of the released sulfide exists in the form of undissociated H_2S before the reaction with Cd^{2+} is observable. The rate of the reaction of cadmium ions with H_2S to release protons according to reaction 9 was followed conductometrically.

$$Cd^{2+} + H_2S \rightleftharpoons CdS + 2H^+ \qquad (9)$$

In the pH range of 4.0–5.3 the rate of release of protons is rather slow (0.1–1 s). Figure 1b shows an example of the evolution of the conductivity signal due to this reaction. The increase in conductivity follows an exponential rate law for at least 3 half-lives. As can be seen in Figure 2, the rate of proton release increases with increasing pH, $[Cd^{2+}]$, or $[HS^-]$ (i.e. dose) in this pH range. The linear dependence on $1/[H^+]^2$ (insert Figure 2a) indicates that the net equilibrium 9 dominates the kinetics, probably through the sequence of equilibria 7, 8, and 10. For the rate to be inversely

$$CdHS^+ \rightleftharpoons CdS + H^+ \qquad (10)$$

proportional to the square of $[H^+]$, all three equilibria have to be rapidly established, relative to the time scales of Figures 1 and 2, yet strongly shifted to the left. The possibility of a direct reaction with S^{2-} can be excluded considering the high value of the second pK_a of H_2S ($pK_{a2} \cong 19$).[17] In order to fit the kinetics of the protons release, computer simulations, including reactions 1–8 and 10 for which the only unknown parameters are K_8 and K_{10}, were performed. As is common in growth kinetics, it was assumed in the kinetic model that all agglomeration reactions of CdS clusters are irreversible and diffusion controlled. In order to obtain the observed signal amplitude (see below) it was also assumed in these calculations that further reactions of RSH with the clusters of 2 or more CdS molecules occur at a diffusion-controlled rate (5×10^9 M^{-1} s^{-1}). An example of these simulations is shown in Figure 1, superimposed on the experimental results. With these assumptions most of the growth occurs by addition of molecules to a small number of clusters. This conclusion is also substantiated by the spectral results described below. These simulations further show that, in order to mimic the experimental observations, either k_8 is much slower than the diffusion limit (assumed 1×10^{10} M^{-1} s^{-1} for this ionic reaction), presumed unlikely, or $K_8 < 5 \times 10^5$ M^{-1}, regardless of the value of K_{10}.

Inspection of the dependence of the final conductivity signal on the various concentrations is quite instructive. As can be deduced from the net reaction 9, two protons are expected to be released from each H_2S created by reactions 1 and 7. The conductivity signal at the end of the growth in Figure 1b indicates a larger number of protons released for each H_2S produced. The final conductivity change, $\Delta\kappa_\infty$, is given in eq 11, where $\lambda_{(i)}$ are

$$\Delta\kappa_\infty = 0.001\{\lambda_{H^+}\Delta[H^+] - 2\lambda_{Cd^{2+}}[CdS]\} \qquad (11)$$

the limiting equivalent conductances of H^+ and Cd^{2+}, taken as 350 and 54 S cm^2 eq^{-1}, respectively (the latter value was assumed in the simulations described above also for the $CdHS^+$ complex). Assuming that all the H_2S produced has reacted with Cd^{2+} at the end of the reaction and that the initial amount of H_2S is equal to the initial concentration of e_{aq}^-, we can substitute $[CdS] = [e_{aq}^-] = G(e_{aq}^-)D$, where $G(e_{aq}^-)$ is the yield of e_{aq}^- (2.7 molecular per 100 eV), and D is the dose in the pulse in units of 100 eV/L. Thus we obtain

$$\Delta\kappa_\infty = 0.001\{n\lambda_{H^+} - 2\lambda_{Cd^{2+}}\}G(e_{aq}^-)D \qquad (12)$$

where n is the number of protons released per H_2S formed by the irradiation. If reaction 9 is the only source of protons, then $n = 2$. In Figure 3, the value of n, calculated from the final conductivity signal with eq 12, is plotted against the initial $[Cd^{2+}]$ for various doses (i.e. $[H_2S]_o$). As can be seen in this figure, the number of protons released exceeds the stoichiometry expected from reaction 9. The same conclusion can be qualitatively reached

(17) Myers, R. J. *J. Chem. Educ.* **1986**, *63*, 687.

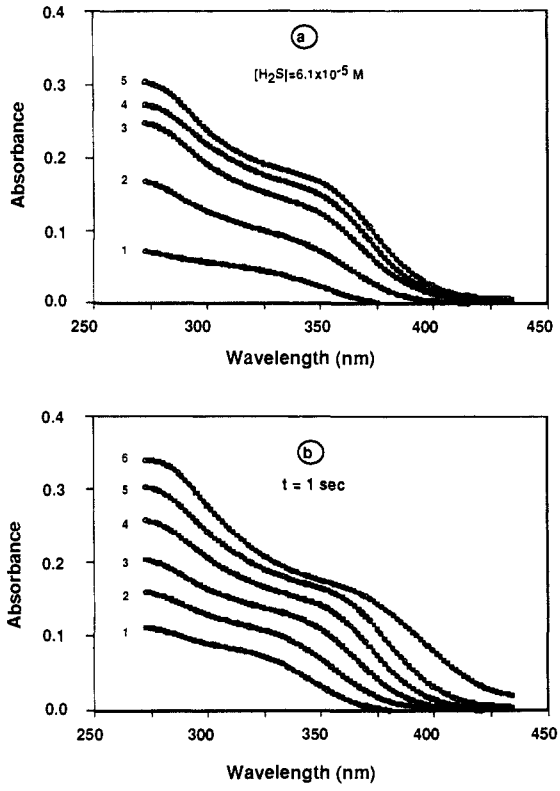

Figure 4. Spectra of growing particles at pH 4.1. $[Cd^{2+}]_0 = 1.0 \times 10^{-4}$ M; [RSH] = 1.0×10^{-2} M. (a) Constant dose ($[H_2S]_0 = 6.1 \times 10^{-5}$ M), at various times after the pulse: 30 ms, 100 ms, 300 ms, 1 s, 3s for 1–5, respectively. (b) At 1 s after the pulse for $[H_2S]_0 = 1.8 \times 10^{-5}$, 2.8×10^{-5}, 4.3×10^{-5}, 6.1×10^{-5}, 8.7×10^{-5}, 2.25×10^{-4} M for 1–6, respectively.

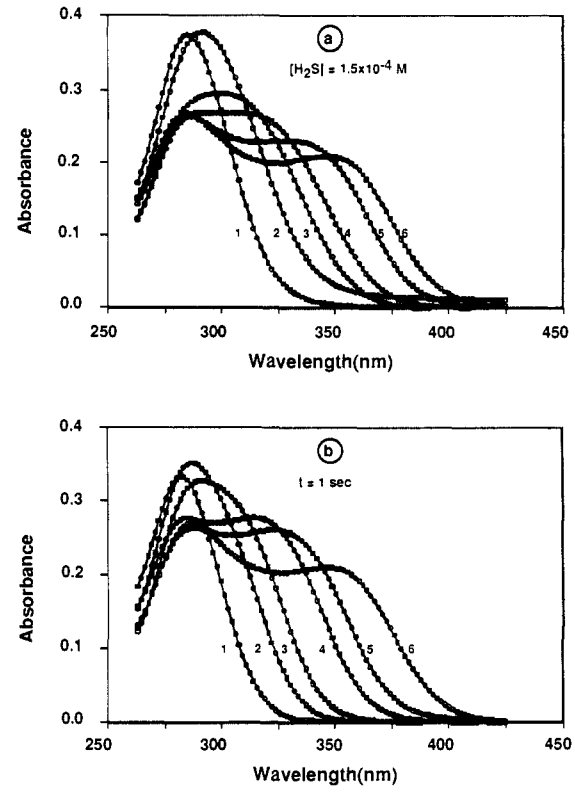

Figure 5. Spectra of growing particles at pH 7.1. $[Cd^{2+}]_0 = 1.0 \times 10^{-4}$ M; [RSH] = 2.0×10^{-3} M. (a) Constant dose ($[H_2S]_0 = 1.5 \times 10^{-4}$ M), at various times after the pulse: 1 ms, 3 ms, 10 ms, 30 ms, 300 ms, 3 s for 1–6, respectively. (b) At 1 s after the pulse for $[H_2S]_0 = 2.1 \times 10^{-5}$, 3.3×10^{-5}, 4.1×10^{-5}, 5.9×10^{-5}, 7.9×10^{-5}, 2.2×10^{-4} M for 1–6, respectively.

from Figure 1 by comparing the initial signal amplitude (corresponding to 1 equiv of HS^- and one H^+) with the final signal amplitude, which is clearly more than twice the initial signal. The highest value observed in Figure 3 is $n = 4.8$. Another source of protons, in addition to reaction 9, must exist in the system. No change in conductivity is expected from the known chemistry of the thiyl radicals on the time scale of Figure 1b, and none was observed in blank solutions containing no Cd^{2+}. Neither was any conductivity change observed in N_2O-saturated solution containing Cd^{2+}, in which all of the primary radicals are converted to thiyl radicals. It appears, therefore, that a reaction of RSH with the CdS particles occurs (reaction 13, where the brackets indicate a CdS cluster) which leads to the release of additional protons. Since at pH 4 no complexation of Cd^{2+} ions to thiol could be

$$\{CdS\} + m\text{RSH} \rightleftharpoons \{CdS\}(RS)_m + mH^+ \qquad (13)$$

observed,[10,14] it may be concluded that RSH is more strongly complexed to CdS particles than to free cadmium ions. It should, however, be noted that eq 13 assumes that no Cd^{2+} ions, in addition to those reacted to form CdS, are involved in complexing RS^-. However, involvement of additional Cd^{2+} ions is most probable considering the high value of n. The existence of polynuclear Cd^{2+}–thiolate complexes in RSH-containing solutions (albeit at higher pHs)[14] is a further indication that this possibility should be considered. Reaction 13a, depicting complexation of RS^- with

$$\{CdS\} + Cd^{2+} + m\text{RSH} \rightleftharpoons \{CdS\}[Cd(RS)m]^{(m-2)-} + mH^+ \qquad (13a)$$

Cd^{2+} ions at the surface of a core cluster of CdS, is one such possibility. These additional cadmium ions are believed to be bound to the crystal lattice of the particles, rather than simply physisorbed.

In the experiments of Figure 3, the number of protons released per each H_2S was found to decrease on increasing the concentration of H_2S, at a given Cd^{2+} concentration, approaching the value of $n = 2$ as $[H_2S]_0$ approaches $[Cd^{2+}]_0$. On increasing $[H_2S]_0$ the particles produced grow to larger sizes, as deduced from the absorption spectra of the particles, with only slight change in their concentration.[10] The surface area per CdS molecule then decreases and hence the relative number of sites available for binding of RSH decreases. More importantly, the concentration of Cd^{2+} ions, free to bind to thiolate according to reaction 13a, decreases with increasing the dose, as the ratio $[H_2S]_0/[Cd^{2+}]_0$ approaches unity. We have also noticed that as these conditions are approached the resultant particles are not as stable as they are when $[H_2S]_0/[Cd^{2+}]_0 \ll 1$. Precipitation occurs then within a few hours. This is a further indication that free Cd^{2+} ions at the particle surface are required for stabilization and growth control by RSH.

On the other hand, n decreases with increasing pH in this range. As the pH increases the fraction of Cd^{2+} ions complexed to RSH in the solution, prior to initiation of the growth, also increases. Reaction 14 then partially replaces reaction 9 and the process may be viewed as a ligand-exchange reaction, with no apparent release of protons:

$$xH_2S + mCd(RS)_2 \rightleftharpoons \{CdS\}_x[Cd(RS)_2]_{m-x} + 2x\text{RSH} \qquad (14)$$

At near neutral pHs the conductivity experiments are impractical. However, when similar experiments were conducted at pH 10, hardly any conductivity change could be observed following the irradiation pulse. At this pH all of the Cd^{2+} ions are complexed and therefore the reaction is an exchange reaction of HS^- with ligated RS^-, i.e. reaction 14 dominates.

c. Absorption Spectra of the Growing Particles and Growth Mechanisms. The changes in the spectra of the solutions following the initiation growth were studied with use of the streak camera detection technique in the 250–500 nm range. Difference spectra collected at pH 4.1 are shown in Figure 4, both as a function of time after the pulse (at constant dose and concentrations) and as a function of the concentration of released H_2S at a fixed time. The spectra are slow to evolve and appear on a time scale similar to that observed in the conductivity experiments for the release

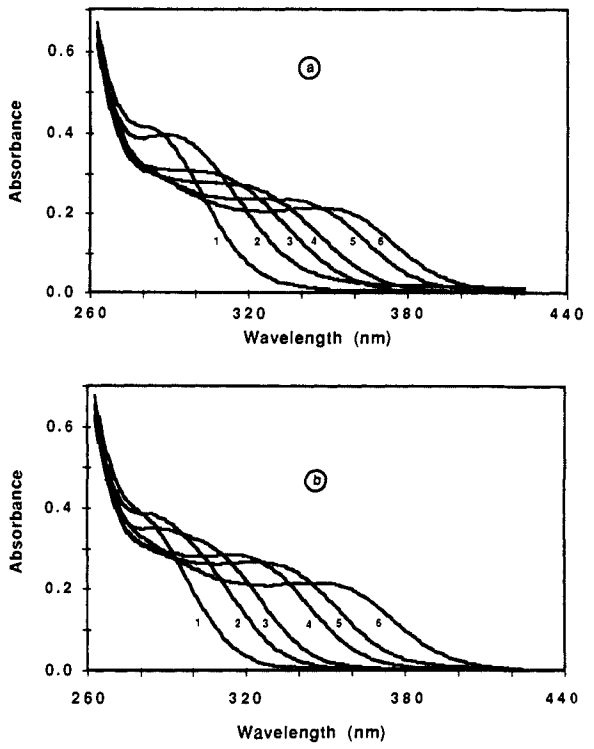

Figure 6. Corrected spectra, assuming complete destruction of the $Cd^{2+}(RS)_2$ complexes that exist in the solution prior to irradiation, for the difference spectra of Figure 5. Numbers correspond to those in Figure 5.

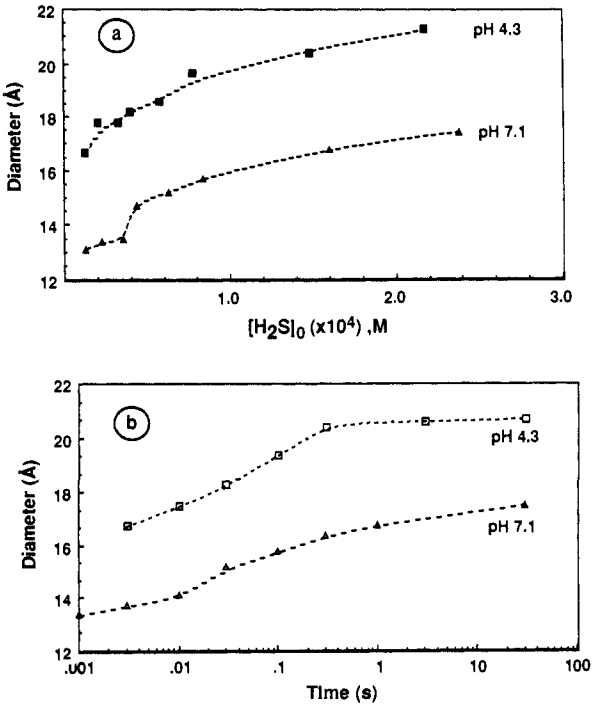

Figure 7. Particle sizes calculated from absorption spectra obtained in solutions containing $[Cd^{2+}]_0 = 1.0 \times 10^{-4}$ M, [RSH] = 2.0×10^{-3} M: (a) for various $[H_2S]_0$ concentrations 1 s after the pulse; (b) as a function of time for $[H_2S]_0 = 1.5 \times 10^{-4}$ M; (△, ▲) pH 7.1; (□, ■) pH 4.3.

of protons. Corresponding spectra, collected at pH 7.1, are shown in Figure 5. At this higher pH all of the Cd^{2+} ions present in the solution are complexed to RS^- in the form of polynuclear complexes.[10,14] These complexes absorb in the UV region (<280 nm),[10] and the difference spectra in Figure 5, therefore, include a component that results from the destruction of the initial complexes. In the absence of quantitative information we assume that the amount of the complexes that was destroyed is equal either to that of $[H_2S]_0$ when $[Cd^{2+}]_0 > [H_2S]_0$ or to $[Cd^{2+}]_0$ when $[Cd^{2+}]_0 < [H_2S]_0$. At the early times of Figure 5a, this may not be correct. Figure 6 shows these corrected spectra for the time evolution of the particles at pH 7.1. When this correction is applied, the spectra at pH 7 are generally similar, although not identical, to those of pH 4. Only slight changes in the absorption spectra were observed at longer times (days) than those shown in Figure 4 and 5. Spectra of stable colloidal solutions of the same system, previously observed following steady state irradiations,[10] are similar to those reported here.

Quantitative information on the growth processes is difficult to obtain from the spectra of Figures 4–6 as the individual absorption spectrum of each of the various cluster sizes is unknown. The problem is further aggravated by the lack of information on the contribution of the Cd^{2+}/RSH complexes at the particle surface. However, the overall shape and position of the spectra in the exciton region provides some qualitative information on the growth mechanism. Comparison between the dose and time dependences of Figures 4–6 reveals a remarkable similarity. Small particles present only at early times in excess H_2S may be stablized for long periods of time by decreasing H_2S concentration (or increasing the thiolate concentration). The correlation between the particle's size and the exciton band in the absortion spectrum of small particles is by now well established. For the presently studied system this correlation has already been verified earlier.[10] Particle sizes calculated from the band observed in the spectra, using the correlation given by Weller et al.,[18] are shown in Figure 7, for pH 4.3 and 7.1, and as a function of time and of $[H_2S]_0$.

Higher pHs, which lead to a higher $[RS^-]/[RSH]$ ratio and thus to increased complexation with Cd^{2+}, lead to smaller particles. At low pHs the earliest spectra observed have their onset at relatively long wavelengths and indicate relatively large particles without any observable spectra that may be attributed to smaller intermediates. As already noted, in the low pH range, complexation of free cadmium ions with thiolate is strongly inhibited. The lack of any observable absorption by very small particles combined with the conductivity results lead to the conclusion that such small particles, which may serve as growth nuclei, exist at the early times only in very low concentration, below the detection limit of our equipment. The growth process detected spectrophotometrically is then primarily a molecule–cluster growth process where equlibrium 9 determines the availability of CdS molecules. A similar growth process was recently invoked for the growth of silver chloride.[12b]

At neutral pH, the absorption band observed at 1 ms hardly shifts during the first 10 ms (Figure 7b). Similarly, at this pH, hardly any growth is observed in the stable particles as $[H_2S]_0$ is increased in the low $[H_2S]_0$ range ($<2 \times 10^{-5}$ M, Figure 7a). Since at this pH all of the original cadmium ions are thiolate bound in the polynuclear complexes, the early CdS cluster are formed within these polymeric complexes. The early spectra (t <10 ms or $[H_2S]_0 < 2 \times 10^{-5}$ M in Figure 6, a or b, respectively) are attributed to these CdS clusters within the Cd^{2+}–thiolate complexes. In this regime the contribution of the latter to the absorption spectra may be dominant. These species were previously observed as stable sols and were labeled "molecular species".[10] The smallest stable particles presently observed at pH 7 (Figure 6) have their shoulder at 290 nm. Species absorbing at shorter wavelength were observed in the steady state experiments at low $[H_2S]_0$. In this range of short wavelengths the corrections necessary in the pulse radiolysis experiments are too large to provide useful information. As time progresses, or at higher $[H_2S]_0$, aggregation of these clusters to larger particles ensues, as the preexisting chains are unable to sustain the larger clusters. The growth process in this regime is then primarily a cluster–cluster process while ripening processes are minimized due to complexation with thiolate ions.

Further indication for different growth mechanisms at the two different pHs can be observed in the dependence of the intensity

(18) Weller, H.; Schmidt, H. M.; Koch, U.; Fojtlk, A.; Baral, S.; Henglein, A.; Kunath, W.; Weiss, K.; Dieman, E. *Chem. Phys. Lett.* **1986**, *124*, 557.

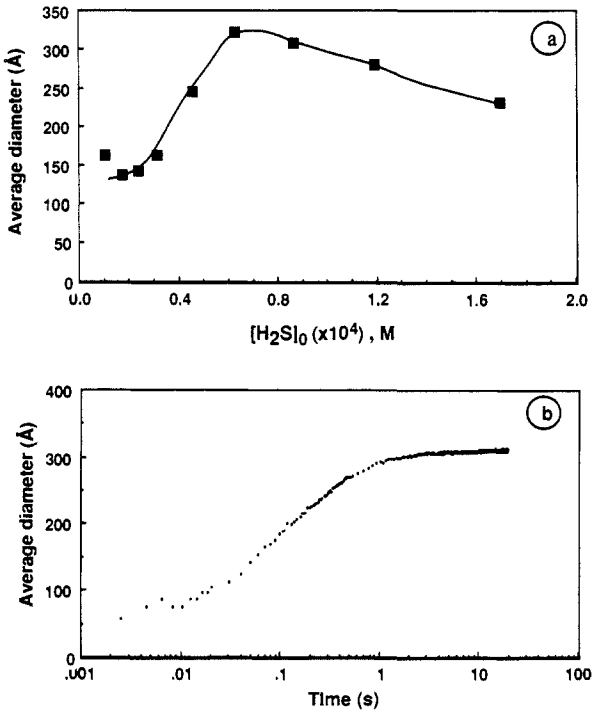

Figure 8. Particle size calculated from light-scattering signals: (a) as a function of $[H_2S]_0$ measured 1 s after the pulse; (b) as a function of time at $[H_2S]_0 = 1.2 \times 10^{-4}$ M. All experiments at pH 4.1; $[Cd^{2+}]_0 = 1.0 \times 10^{-4}$ M; [RSH] = 1.0×10^{-2} M.

of absorption on time. While at the low pH the absorbance increases monotonically with time, it decreases with time at neutral pH. In the range of quantum size particles the intensity of absorption of the exciton band is proportional to the number of particles.[19] If the total mass remains constant as a function of time in the experiments of Figure 5a, the number of particles must decrease as the particle grow, leading to the decrease in absorbance at the exciton band region. The increase in the intensity of absorption in Figure 4a therefore indicates an increase in the number of particles that contribute to the absorption as more material is converted to CdS, in agreement with a cluster–molecule growth mechanism. The latter mechanism also leads to broader size distribution than a cluster–cluster mechanism. This is reflected in the narrower absorption bands observed at neutral pH than at low pH.

d. Sizes from Light Scattering. Several experiments to measure particle sizes from light scattering were performed. At neutral pH no light-scattering signal above the background level could be observed following the irradiation pulse. This is to be expected since the sizes calculated from the absorption spectra are below the detection limit of the light-scattering technique used. On the other hand, at pH 4.1 strong scattering signals were observed. These signals, converted to sizes assuming complete conversion of HS^- to CdS,[12] are shown in Figure 8. These sizes are about an order of magnitude larger than those calculated from the band in the absorption spectra. When the stabilizer hexametaphosphate (HMP) was added to the solutions (1×10^{-4} M) prior to irradiation, no light-scattering signal could be observed following the irradiation at pH 4.1. Parallel experiments on the absorption spectra of the growing particles in the presence of HMP also indicated slower growth rate and somewhat smaller particles relative to identical experiments in the absence of HMP.

Several factors may contribute to the discrepancy between the sizes calculated from the light-scattering results and those obtained spectrally. Sizes determined from light scattering represent a volume weighted average volume and therefore are strongly skewed toward larger particles. Sizes determined from spectra reflect number averaging and are therefore strongly weighted toward the particles of larger populations. Only for very narrow size distributions will the two methods coincide. As previously noted[10] and as is evident from the width of the lowest energy absorption band in Figure 4, a rather broad size distribution is obtained at pH 4. In addition, our TEM results indicate extensive clustering of small particles on the microscope grids, while maintaining clear boundaries of the component particles. If such aggregates occurs also in solution, the large aggregates will be detectable by light scattering while their contribution to the absorption will still maintain the spectroscopic properties of the individual particles. To substantiate the possibility that clustering to large aggregates does not necessarily lead to loss of the small component particles we induced coagulation of the small particles by addition of 0.1 M $NaClO_4$ to a sol prepared at pH 4 (no stabilizers). The precipitated colloid was pale yellow in color and upon redispersion at pH 4 showed essentially the same absorption spectrum as prior to the precipitation. Evidently, the small particles maintained their spectroscopic identity even after precipitation and redispersion.

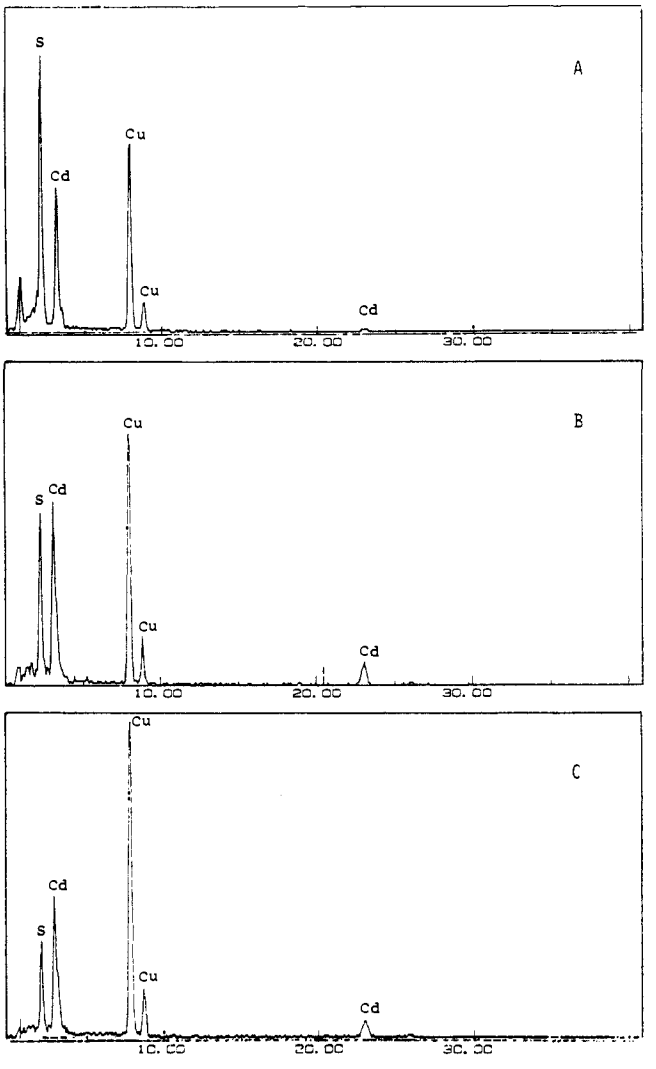

Figure 9. Elemental analysis by EDAX of the particles under the microscope. Specimen deposited from solutions of the same concentration as in Figure 8: (a) at pH 7.1; (b) at pH 4.3; (c) chemically prepared by injection of H_2S to Cd^{2+} solution in the absence of RSH.

e. Electron Microscopy. Particles of various sizes, obtained by controlling the relative $[RSH]/[H_2S]_0$ ratio, were examined by TEM, electron diffraction, and energy dispersive X-ray fluorescence (EDAX). Nearly spherical particles of sizes in the range of 20 to 100 Å, depending on $[H_2S]_0$, with extensive aggregation upon precipitation on the microscope grids, were observed by TEM. The extent of aggregation could be reduced by

(19) Rossetti, R.; Ellison, J. L.; Gibson, J. M.; Brus, L. E. *J. Chem. Phys.* **1984**, *80*, 4464.

Scheme I

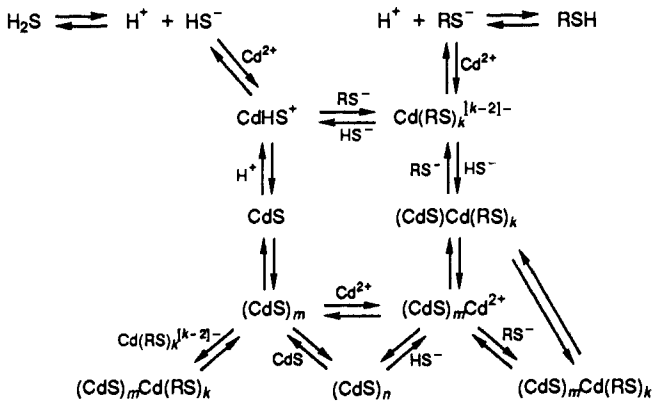

dilution of the solution prior to deposition on the grids or by further addition of external stabilizers. Diffraction patterns for all preparations show the cubic β-CdS structure. Results from EDAX experiments are shown in Figure 9, where the ratio of sulfur/cadmium signals from specimens deposited following irradiation at pH 7.1 and 4.3 are compared with those of a specimen deposited from chemical preparation of CdS in the absence of RSH. It is clear from Figure 9 that the sample prepared at pH 4.3 is slightly enriched in sulfur while the one prepared at pH 7.1 indicates substantial increase in sulfur content. This is in accordance with the above discussion where the sulfur-to-cadmium ratio may be expected to increase due to complexation of thiolate at the surface.

Conclusions

The essential features of the mechanism for CdS growth, controlled by RS^-, which emerges from this study, are outlined in Scheme I. The end products at the bottom right and left sides of the scheme represent the CdS core with the cadmium–thiolate complexes covalently bound to the surface. The subscript k is used to indicate the possibility of polynuclear complex formation with both free Cd^{2+} ions in solution and at the surface. The effect of pH appears through the acid–base equilibria of H_2S and RSH. The important step for control of the growth is provided by the competition between RS^- and HS^- for the Cd^{2+} ions at the surface of the growing particle. The left-side branch of the scheme dominates at low pHs when thiolate complexation of free Cd^{2+} is minimal. The right side dominates at higher pHs and includes the growth of CdS clusters bound to the polynuclear complexes.

Two main advantages of the thiolate controlled growth can be indicated at this point. The ability to externally control the growth and the final size of the particles simply by adjusting the relative $Cd^{2+}/RSH/H_2S$ concentrations is one obvious appealing feature. No less significantly is the ability to control, and modify, the surface properties of the particles through use of a variety of derivatized thiols in such systems. It is the strong binding of the cadmium ions to both the CdS lattice and the thiol that provides this route for surface modification. Interestingly the recent observation of cadmium bio-mineralization in the form of CdS probably operates via a similar mechanism.[20]

Acknowledgment. The dedicated operation of the linac by D. Ficht and G. Cox is much appreciated. This work was performed under the auspices of the Office of Basic Energy Sciences, Division of Chemical Science, US-DOE, under contract No. W-31-109-ENG-38.

(20) (a) Dameron, C. T.; Reese, R. N.; Mehra, R. K.; Kortan, A. R.; Carroll, P. J.; Steigerwald, M. L.; Brus, L. E.; Winge, D. R. *Nature* **1989**, *338*, 596. (b) Reese, R. N.; Winge *J. Biol. Chem.* **1988**, *263*, 12832.

Synthesis, Luminescence, and Excited-State Complexes of the Tris(1,10-phenanthroline)- and Bis(terpyridine)iridium(III) Cations

N. P. Ayala,[1] C. M. Flynn, Jr.,[2] LouAnn Sacksteder,[3] J. N. Demas,*[,3] and B. A. DeGraff*[,4]

Contribution from the Departments of Chemistry, University of Virginia, Charlottesville, Virginia 22901, and James Madison University, Harrisonburg, Virginia 22807.
Received September 18, 1989

Abstract: We report the synthesis and luminescence properties of $Ir(phen)_3^{3+}$ and $Ir(terp)_2^{3+}$ (phen = 1,10-phenanthroline and terp = 2,6-bis(2-pyridyl)pyridine). Their emissions are assigned to predominantly π–π^* phosphorescences. A novel excited-state complex is proposed to form between $Ir(phen)_3^{3+}$ and $Ir(terp)_2^{3+}$ and $HgCl_2$. Although $HgCl_2$ is normally a quencher, it can greatly enhance the lifetimes and luminescence efficiencies of the $Ir(phen)_3^{3+}$ and $Ir(terp)_2^{3+}$—up to an order of magnitude. The changes arise from alteration of the radiative and nonradiative rate constants in the excited-state complex. The effect of temperature, solvent, oxygen, and inert ions on the interactions of $HgCl_2$ with the excited complexes is explored. A simple associative model accurately reproduces all lifetime and intensity changes. A rationale based on the well-known affinity of $HgCl_2$ for aromatic molecules is proposed.

The photochemistry and photophysics of platinum metal complexes have played a pivotal role in attempts to develop new solar energy conversion and photocatalytic systems.[5] Among this group, the complexes of Ir(III) with α-diimine ligands have particularly complex chemistry and photophysics.[6-9] In particular, $Ir(bpy)_3^{3+}$

(1) Current affiliation: Westwood Chemical Corp., Middeltown, NY 10940.
(2) Current affiliation: U.S. Bureau of Mines, Reno, NV.
(3) University of Virginia.
(4) James Madison University.

(5) (a) *Energy Resources through Photochemistry and Catalysis*; Grätzel, M., Ed.; Academic Press: New York, 1983. (b) Kalyanasundaram, K. *Coord. Chem. Rev.* **1982**, *46*, 159. (c) Balzani, V.; Bolletta, F.; Gandolfi, M. T.; Maestri, M. *Top. Curr. Chem.* **1978**, *75*, 1. (d) Kalyanasundaram, K. *Photochemistry in Microheterogeneous Systems*; Academic Press, 1987.
(6) DeArmond, M. K.; Carlin, C. M. *Coord. Chem. Rev.* **1981**, *36*, 325.

0002-7863/90/1512-3837$02.50/0